

MASTER

Modelling, analysis and design of a MEMS resonator based oscillator system

Padhye, K.P.

Award date:
2008

[Link to publication](#)

Disclaimer

This document contains a student thesis (bachelor's or master's), as authored by a student at Eindhoven University of Technology. Student theses are made available in the TU/e repository upon obtaining the required degree. The grade received is not published on the document as presented in the repository. The required complexity or quality of research of student theses may vary by program, and the required minimum study period may vary in duration.

General rights

Copyright and moral rights for the publications made accessible in the public portal are retained by the authors and/or other copyright owners and it is a condition of accessing publications that users recognise and abide by the legal requirements associated with these rights.

- Users may download and print one copy of any publication from the public portal for the purpose of private study or research.
- You may not further distribute the material or use it for any profit-making activity or commercial gain

Modelling, Analysis and Design of a MEMS Resonator based Oscillator System

by

K.P. Padhye

Master of Science thesis

Project period: October 2008

Report Number: 08A/11

Commissioned by:

Prof.dr.ir. P.P.J. van den Bosch

Supervisors:

Dr.ir.J.J. Koning (NXP Semiconductors)

Ir. J.J.M. Bontemps (NXP Semiconductors)

Modelling, Analysis and Design of a MEMS Resonator based Oscillator System

Kaustubh P. Padhye

Abstract— Significant progress has been made in the field of silicon technology over the past few decades, which has enabled chip designers to make chips smaller and integrate different functional blocks on a single chip. However the quartz crystal, a peripheral of the chip, which provides accurate timing reference for the chip to operate, remains non-integral in the existing technology. MEMS resonators, which are considered a promising alternative for replacing quartz crystal can be integrated on chip and also have smaller foot print on silicon. To commercialize these MEMS resonators for electronic applications, it is important to have an accurate electrical model of these mechanical systems. In this paper an electrical model of a capacitive MEMS resonator is presented. The resonator is characterized and the dependencies of the model parameters are studied. Further the resonator model is used to design a single chip system in package MEMS oscillator to operate at a frequency of 25.85 MHz. The MEMS oscillator presented in this paper acts as stepping stone that opens the possibilities of integrating mechanical systems along with electrical systems on a single chip platform.

However most of the MEMS oscillators developed are a two chip oscillator design i.e. resonator is fabricated on one chip and the amplifier is fabricated on another chip. The availability of the existing fabrication technologies and the introduction of new processing methods have enabled us to develop a single chip MEMS oscillator that is presented in this paper. To develop an electronic system consisting of a mechanical device it is important to have an accurate electrical equivalent model of this mechanical element, so that further electronic circuitry can be designed based on the electrical response of the mechanical system so as to satisfy the functional requirements of the electromechanical system. In this paper section II describes the process used to fabricate these resonators. In section III and section IV the modeling and the measurements of the MEMS resonator are presented. Section V explains the challenges of designing MEMS oscillator based on the principle of capacitive readout and different solutions are proposed and in section VI conclusion from the study are discussed along with recommendations for future work.

I. INTRODUCTION

Almost all modern day electronic systems need a reference frequency to synchronize with other subsystems and systems. The clock signal in an electronic system is analogous to a heartbeat of a human body. Since the past few decades quartz crystals have been providing an accurate timing and frequency references for frequency-controlled world [1]. With the development of new silicon technologies chips have become smaller and more discrete components and functionalities are being integrated on chip. The quartz crystal remains the only non-integral component in the in the existing technology. Researchers have tried to find a solution to this problem by utilizing mechanical resonance phenomenon to develop micro mechanical silicon resonators. These resonators open up enormous possibilities to create miniature scale wireless communication devices [2]. These devices typically have a quality factor, which ranges from 10^3 to 10^4 for an eigen frequency around 10 MHz [3, 4, 5]. These MEMS resonators have been considered as an attractive replacement for a quartz crystal due to their small size (small footprint on silicon), potential for fabrication and compatibility with standard CMOS and VLSI processing [6]. The MEMS oscillators satisfying the phase noise specification for the GSM standard have already been reported [7].

II. RESONATOR DESIGN AND FABRICATION

A. Processing of SOI MEMS Resonator

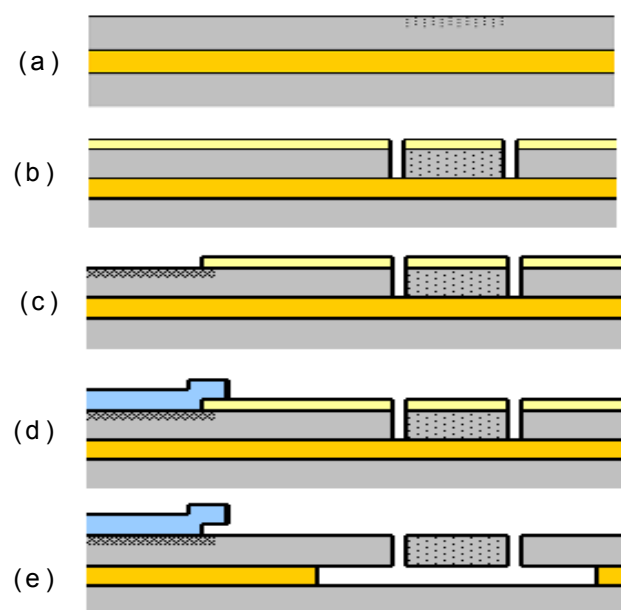


Fig. 1 Process steps for fabricating MEMS resonators on SOI wafers.

The MEMS resonators are fabricated on SOI (Silicon on Insulator) wafers. The top layer is a 1.5 μm single crystal silicon layer in which the MEMS resonators are fabricated. The second layer is a 1 μm insulating layer of SiO_2 . The third layer is again single crystal silicon layer approximately 700 μm thick, which forms the substrate. The choice for this very thin SOI device has been given in [8].

The process used to fabricate SOI MEMS resonators consists of the following steps and is shown in Fig 1.

- Selective doping: The top layer of silicon is selectively doped to improve the conductivity of the resonator and the electrodes.
- Trench etch: Narrow trenches are etched in the SOI using standard lithography steps.
- Contact implantation: To improve the conductivity of the surface where the contacts with the metal are made a surface dope is added.
- Aluminum deposition: Aluminum is deposited to create bond pads and the wires.
- SiO_2 or BOX etch: In this step the SiO_2 layer is etched using a HF vapour.

The two designs of the MEMS resonators are shown in Fig 2. The resonators have been fabricated using the described process flow.

B. Designs of the MEMS Resonator

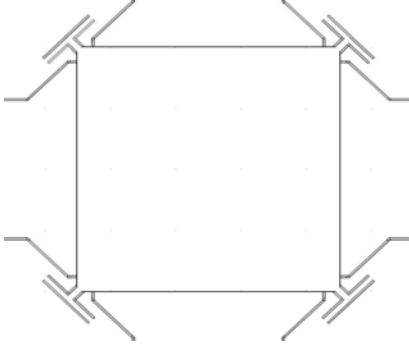


Fig. 2 (a) Layout of a square plate resonator

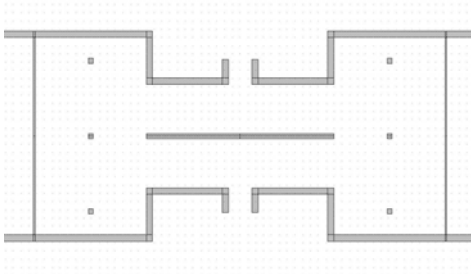


Fig. 2 (b) Layout of a dogbone resonator

Both the designs shown in Fig. 2(a),(b) use the electrostatic force for actuation whereas the detection principle used for detecting the resonance signal is different for the two designs.

In case of the square plate resonator, capacitive detection is used for detecting the resonance signal. In case of a dogbone resonator a piezoresistive detection principle is used. The choice for the detection principle is based on the geometry and the design of the structure. Details about the actuation and detection principles along with model are explained in the next section.

III. MEMS RESONATOR MODEL

A. Lumped parameter model

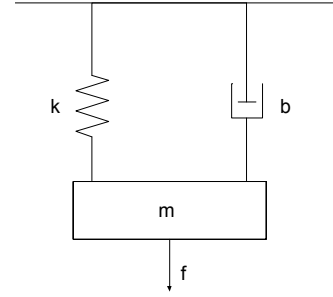


Fig 3 Mass spring and a damper system used to model the MEMS resonator.

The MEMS resonator comprises of a freestanding element (square plate or a dogbone), which can resonate in different eigen modes. Based on the type of actuation used, a particular eigen mode is selected. A layout of the resonator is shown in Fig 2. To understand the operation of the resonator an analytical model is developed where a mechanical resonator is modeled as a mass, spring and damper system as shown in Fig 3. From the eigen mode in which the structure resonates the eigen frequency is determined.

The equation of motion of a linear one-dimensional model of a MEMS resonator with damping is given by

$$f(t) = m\ddot{x}(t) + b\dot{x}(t) + kx(t) \quad (1)$$

Where $f(t)$ is the force acting on the mechanical system, m is the mass of the system, k is the spring constant while b is the damping coefficient. If $f(t)$ is assumed to be sinusoidal it can be written as:

$$f(t) = Fe^{j\omega t} \quad (2)$$

Since the force acting on the resonator is sinusoidal the displacement is also sinusoidal and is given by:

$$x(t) = Xe^{j\omega t + \phi} \quad (3)$$

From equation (3) the values of $\dot{x}(t)$ and $\ddot{x}(t)$ are derived

$$\dot{x}(t) = j\omega Xe^{j\omega t + \phi} \quad \text{and} \quad \ddot{x}(t) = -\omega^2 Xe^{j\omega t + \phi} \quad (4)$$

Substituting equation (3) and (4) in equation (1) gives

$$X = \frac{Fe^{-j\phi}}{j\omega} \left[j\omega m + b + \frac{k}{j\omega} \right]^{-1} \quad (5)$$

From the geometry of the structure it can be approximated that the outer end of the plate and the electrode form a parallel plate capacitor. The resonators are actuated using an electrostatic force. The electrostatic force applied over the gap is given by the following equation.

$$F = \frac{dE}{dx} \quad (6)$$

Where, E is the energy stored in the capacitor and is given by

$$E = \frac{1}{2} CV^2 \quad (7)$$

Where, C is the value of the capacitance in farad and V is the voltage across the plates.

Substituting equation (6) in equation (7) gives the following

$$F = \frac{1}{2} \frac{dC(x)}{dx} V^2 \quad (8)$$

Applying the principle of superposition the resultant voltage V(t) is given by

$$V(t) = V_{dc} + V_{ac} e^{j\omega t} \quad (9)$$

By substituting equation (9) in equation (8) gives the following

$$F = \frac{d}{dx} \frac{\epsilon_0 wh}{(g-x)} V_{dc} V_{ac} \quad (10)$$

Since, the term V_{ac}^2 is very small it can be neglected. The term V_{dc}^2 provides a constant force on the resonator. This force being steady force cannot bring the structure into resonance. The only term, which contributes towards the applied electrostatic force, is the combination of the V_{ac} and V_{dc} . Thus in equation (10) V^2 can be approximated as follows

$$V^2 \approx (2V_{dc})V_{ac} \quad (11)$$

Equation (10) gives the electrostatic force used for actuation. Where, w is the width of the resonator in meter, g is the width of the transduction gap in meter and $h=1.5\mu\text{m}$ is the thickness of the SOI layer in which the resonators are designed. $\epsilon_0 = 8.85\text{e-}12$ [F/m] is the permittivity of free space. A parameter η is introduced which is the electromechanical coupling coefficient of the system. It is the factor that relates the electrical driving ac voltage (force) to the mechanical force on the resonator. Since, the maximum displacement of the resonator x , is very small as compared to the gap width g , ($x \ll g$) the term $(g-x)$ can be approximated by g .

$$\eta = \frac{\epsilon_0 wh V_{dc}}{g^2} \quad (12)$$

The ac component of the electrostatic force as a result of the applied ac voltage is given by

$$F = \eta V_{ac} \quad (13)$$

For a parallel plate capacitor the voltage over the gap induces a net negative charge on one plate and net positive charge on the other plate since $V_{ac} < V_{dc}$.

$$q = CV = \frac{\epsilon_0 wh}{(g-x)} V_{dc} \quad (14)$$

Movement of the resonator under the influence of the force causes a variation in the gap width. This movement causes a variation of charge q over the gap as a result current is induced through the resonator. This is the principle of capacitive detection. The induced current is proportional to the velocity of the resonator and can be written as

$$I = \frac{dq}{dt} = V_{dc} \frac{\partial C}{\partial x} \frac{\partial x}{\partial t} = \eta \frac{\partial x}{\partial t} = \eta \dot{x} \quad (15)$$

The term η relates the velocity of the resonator in mechanical domain to the flow of current in electrical domain.

Considering the equivalence between power in mechanical domain and the electrical domain gives

$$P_{mech} = f(t) \cdot v(t) \quad (16)$$

$$P_{elect} = V_{ac}(t) \cdot I_{ac}(t) \quad (17)$$

By relating the mechanical power to the electrical power

$$f(t) \cdot v(t) = V_{ac}(t) \cdot I_{ac}(t) = \frac{V_{ac}^2(t)}{Z} \quad (18)$$

$$F \cdot e^{j\omega t} \cdot (j\omega X e^{j\omega t + \phi}) = F e^{j\omega t} \cdot j\omega e^{j\omega t + \phi} \cdot X \quad (19)$$

By substituting X from equation (5) we have

$$F^2 e^{2j\omega t} \left(j\omega m + b + \frac{k}{j\omega} \right) = \frac{V_{ac}^2 \cdot e^{2j\omega t}}{Z(\omega)} \quad (20)$$

Substituting equation (12) in equation (18) we have

$$Z(\omega) = \frac{1}{\eta^2} \left(j\omega m + b + \frac{k}{j\omega} \right) \quad (21)$$

In case of an electrical resonance a R-L-C circuit can be considered where the equation of impedance of the circuit is given by

$$Z_{RLC}(\omega) = R_m + j\omega L_m + \frac{1}{j\omega C_m} \quad (22)$$

By comparing equation (18) and equation (19) equivalence between the parameters from mechanical domain and parameters from electrical domain is established.

$$\begin{cases} R_m = \frac{b}{\eta^2} = \frac{\sqrt{km}}{Q\eta^2} \\ L_m = \frac{m}{\eta^2} \\ C_m = \frac{\eta^2}{k} \end{cases} \quad (23)$$

In equation (22) Q is the Quality factor of the resonator.

The above equations show how the mechanical parameters relate to the electrical parameters. The square plate resonator shown in Fig 2 (a) can be modeled using equation (23). Fig. 3 shows the electrical equivalent model of the capacitive resonators. One of the advantages of the capacitive resonator is that, there is no power dissipation in the resonator thus; it can be used for low power applications. The resonators based on the capacitive detection operate at high bias voltages.

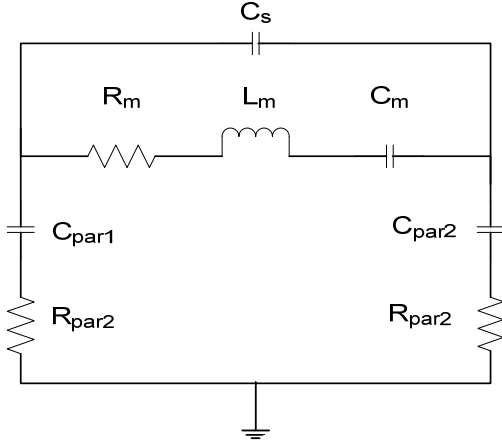


Fig. 4. Electrical Equivalent of a MEMS resonator

In case of a dogbone resonator as shown in Fig. 2 (b) the actuation principle remains the same whereas the detection principle differs. In case of the dogbone resonator the piezoresistive property of silicon is utilized to detect the resonance signal. A current source is used to force a constant current through the structure. Due to the movement of the resonator the resistance of the resonator changes which in turn changes the voltage over the resonator. The output signal in case of piezoresistive detection is given by the following equation.

$$V_o = I_d f(R) \quad (24)$$

Where V_o is the output signal in volts, I_d is the current forced through the resonator and $f(R)$ is the function that defines the modulation in the resistance of silicon due to the movement of the structure. The advantage of this detection principle is that the signal level at the output is much higher as compared to capacitive detection since, it depends on the current forced through the structure. From equation (24) it can be seen that by increasing the current through the resonator the resonance signal increases at the same time the power dissipation in the resonator increases that is the disadvantage of this detection principle. The model of the piezoresistive MEMS resonator is explained in more detail in [9].

IV. MEASUREMENT OF MEMS RESONATOR

A. Measurement challenges

The electrical characterization of the MEMS resonator cannot be done in a trivial way; it requires a measurement setup, which overcomes the following challenges.

- The impedance of the MEMS resonators is very high, typically above 500 k Ω , which makes the signal transmission levels low making it difficult to measure resonance response of the device.
- The response of the MEMS resonators is strongly damped by gas when measured at a pressure above 1 mbar [10].

- The parasitic impedance at resonance frequency is low which lowers the value of resonance signal and decreases the signal to noise ratio of the resonator.
- MEMS resonators are measured at high bias voltages as high as 80 V. These voltages are typically applied over a gap of 200 nm these makes it important to protect the rest of the circuitry from high voltage.

B. Measurement setup

The response of the MEMS resonator has been measured using the measurement setup as shown in Fig. 5. A high dc voltage is applied over the narrow gap to generate the actuating force. Bias tees (protection devices) have been used in order to protect the network analyzer from the high dc voltages. The 1 M Ω resistances prevent damage to the device and protect the user by limiting the current when the electrodes and the resonator get shorted. The network analyzer is used to measure the response of the resonator.

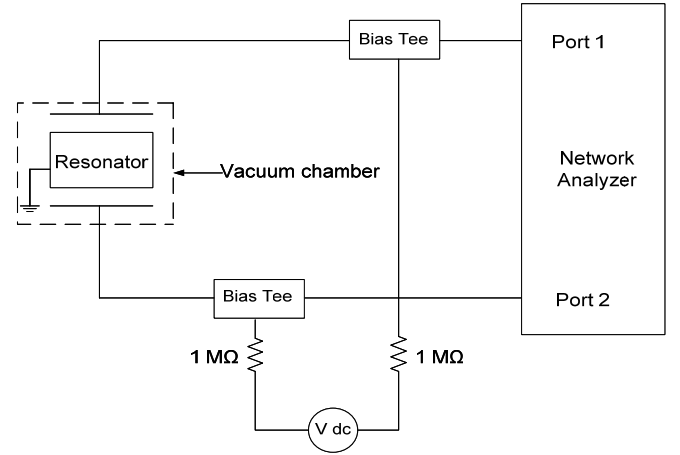


Fig. 5 Measurement setup used to measure the response of MEMS resonators

For measuring the response of a two port network such as a resonator, which operates at high frequencies, S-parameter measurement is preferred over other parameters like H, Y, Z etc. The main advantage of S-parameter measurement over the other parameter measurement is that, in case of a S-parameter measurement the ports of the network are not required to be opened or shorted like in case of other parameters which poses a serious practical difficulty for measuring high frequency response of a network. More information about S-parameter measurement can be obtained in the Appendix.

The response of the resonator is damped due to the presence of air molecules, which lowers the Quality-factor of the resonator [11]. From experiments it has been observed that below the pressure of 10^{-2} mbar the damping due to air molecules is not the dominant damping mechanism. In order to eliminate the effect of air damping the measurements have been performed by placing the resonator in a vacuum chamber with pressure below 10^{-2} mbar.

B. Validation of the proposed model

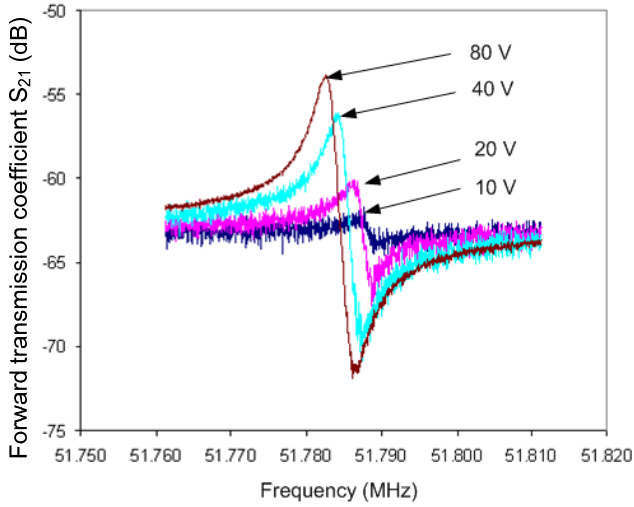


Fig. 6 Measured forward transmission coefficient S_{21} of the resonator. Arrows indicate different bias voltages used during measurement.

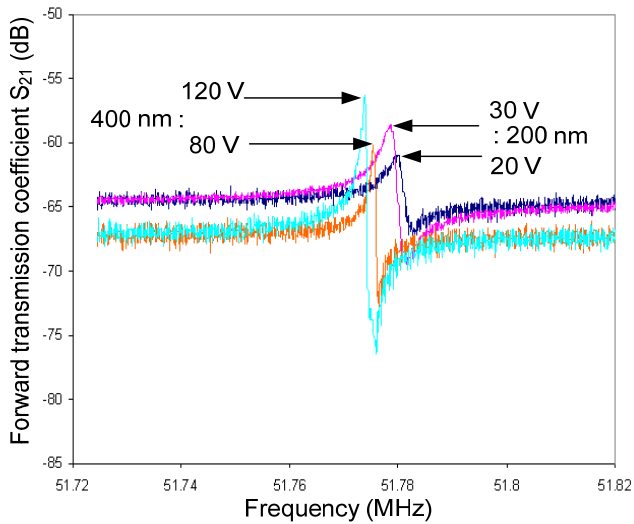


Fig. 7 Measured forward transmission coefficient S_{21} of the resonator having different gap widths between electrode and resonator. Arrows indicate different bias voltages used during measurement for different gap width

To validate the proposed lumped parameter model different sets of measurements have been carried out on the resonator. By performing different experiments the effects of change of parameters such as dc bias voltage and variation of gap width between the resonator and the electrodes on the S-parameters of the resonators have been observed. These results are as shown in Fig. 6 and Fig. 7. With the increase in the value of the bias voltage the resonance peak increases. This effect is due to the increase in the value of the electromechanical coupling coefficient η . Increase in η lowers the value of the motional resistance R_m , and is in accordance with the results predicted using the lumped parameter model. In the second experiment two resonators having different gap width between the electrode and the plate have been measured

keeping the electromechanical coupling coefficient constant, it has been observed that the signal level outside resonance peak is lowered due to decrease in the value of the shunt capacitance C_s .

D. Parameter extraction and Electrical model of the Resonator

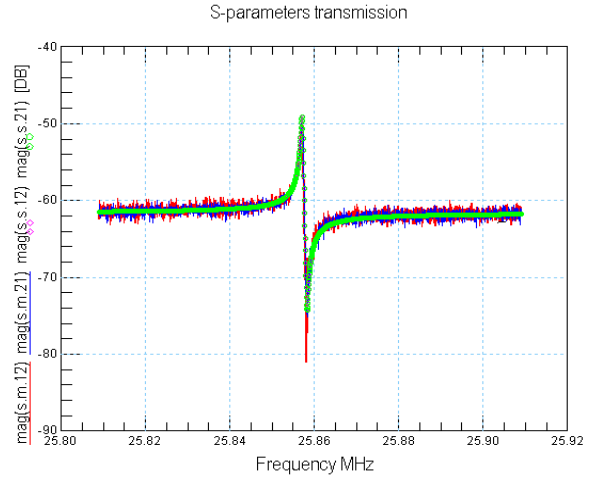


Fig. 8 Data fit of measured and simulated for transmission parameter magnitude response of the resonator using the electrical equivalent model

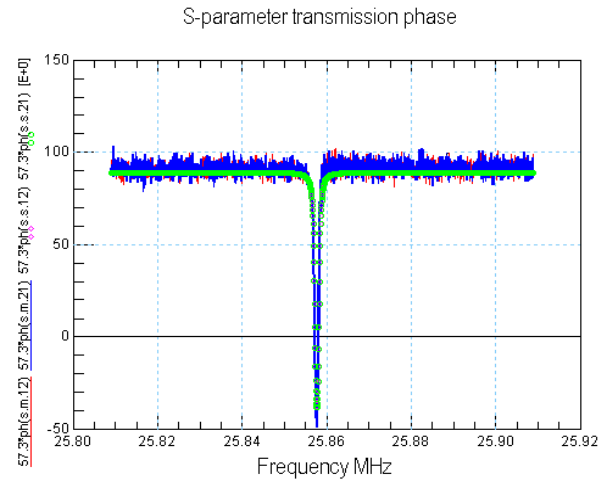


Fig. 9 Data fit of measured and simulated for transmission parameter phase response of the resonator using the electrical equivalent model

An electrical model consisting of the lumped parameters has been built in an electrical simulator. The S-parameter data is imported to the simulator and by tuning the model parameter an optimal fit is obtained. To fit all the sets of S-parameters components other than the motional parameters namely $R_{par 1}$, $R_{par 2}$, $C_{par 1}$, $C_{par 2}$ and C_s are added. The first four components are known as parasites. By tuning these parasites the fits for input reflection coefficient and the output reflection coefficient are obtained. The fifth component C_s is known as the shunt capacitance. When all the data fits are optimized the values of the motional parameters, shunt

capacitance and the parasites are obtained. The electrical equivalent of the MEMS resonator is as shown in Fig. 4. The extracted values of the motional parameters are compared with the values obtained from the finite element simulation. Fig. 10 shows the comparison of the values of the motional parameters obtained from the finite element simulation and from the electrical equivalent model and their dependency on the bias voltage.

E. Comparison of extracted parameters and the physical parameters.

TABLE I
RESONATOR DIMENSIONS USED FOR FINITE ELEMENT SIMULATION

Parameter	Symbol	Value	Units
Resonator side length	L	161.5	[μm]
Resonator height	H	1.5	[μm]
Transduction gap	G	200	[nm]

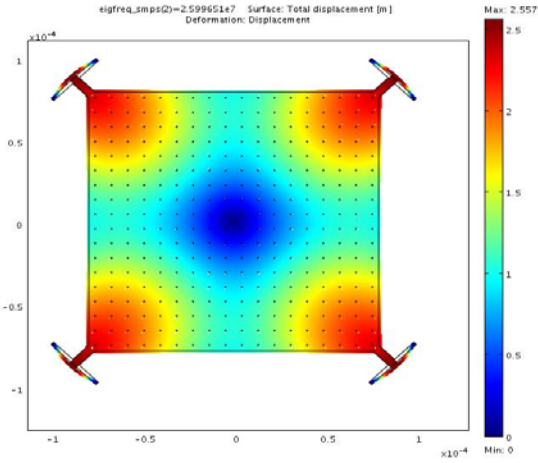


Fig. 10 Displacement of the structure obtained from finite element simulation

The geometry of the structure has been defined in a finite element simulator based on the values mentioned in Table.1. From the eigen frequency simulation the eigen mode corresponding to the eigen frequency of 25.99 MHz has been selected. Fig. 10 shows the results of the eigen frequency simulation. Different colours correspond to the displacement of the elements of the structure. From the eigen frequency simulation the total energy E stored in the structure is obtained. Similarly the total displacement of the structure x obtained. From the following equation the spring constant k is obtained.

$$E = \frac{1}{2} k x^2 \quad (25)$$

From the value of the spring constant and the resonance frequency the value of the effective mass is calculated.

$$m = \frac{k}{4\pi^2 f_o^2} \quad (26)$$

Using the values of k and m and equation (23) the values of the motional parameters have been calculated.

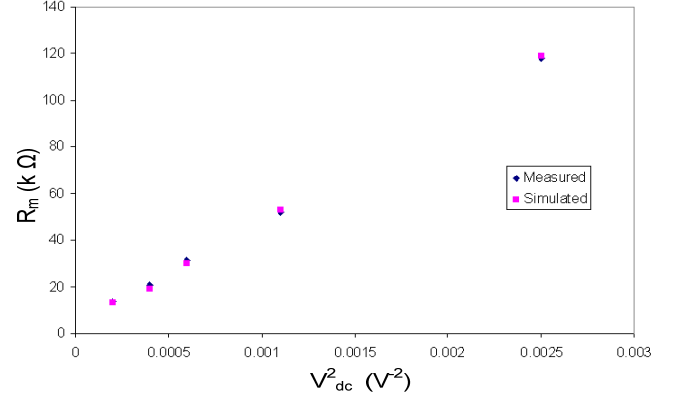


Fig. 11(a) Comparison of the value of R_m obtained from finite element simulation and from parameter extraction using the electrical equivalent model. The plot shows relative scaling of the motional parameter with bias voltage.

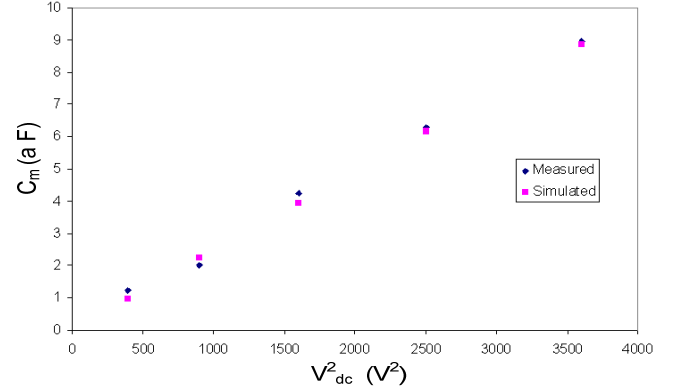


Fig. 11(b) Comparison of the value of C_m obtained from finite element simulation and from parameter extraction using the electrical equivalent model. The plot shows relative scaling of the motional parameter with bias voltage.

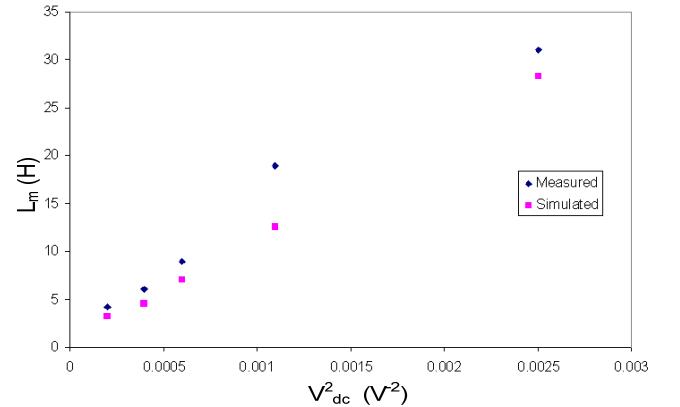


Fig. 11(c) Comparison of the value of L_m obtained from finite element simulation and from parameter extraction using the electrical equivalent model. The plot shows relative scaling of the motional parameter with bias voltage.

From the lumped parameter model it can be seen that the

values of motional resistance and inductance vary linearly with the inverse square of the bias voltage whereas the values of C_m vary linearly with the square of bias voltage. Fig. 11(a), (b), (c) show the scaling of the parameters with the bias voltage. The linear trend observed in the plots is in accordance with the trend predicted from the lumped parameter model. From the figures it can be seen that the motional parameters obtained from measurement and simulation show a good match. Thus, from the results discussed in the previous section and this section the electrical equivalent model of the mechanical system is successfully validated.

V. DESIGN OF MEMS OSCILLATOR

A. Theory of Oscillator

The MEMS resonators have been characterized and an electrical equivalent model of the resonator discussed in the previous section is used as a starting point for the oscillator design. An electronic oscillator consists of mainly two components, the amplifier and a frequency-determining network, which are cascaded together as shown in the Fig. 12. In case of design of a MEMS oscillator the highly selective frequency response of the resonator is used as a frequency-determining network.

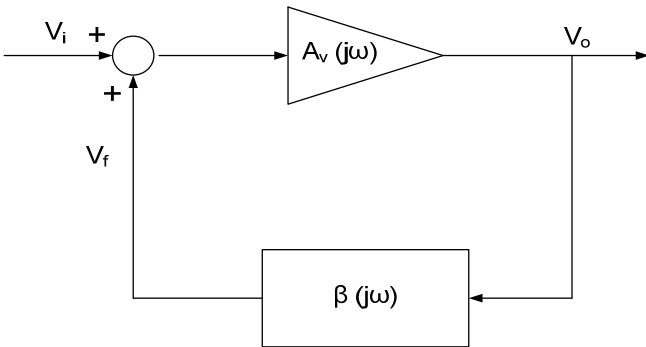


Fig. 12. Block diagram of a MEMS resonator based Oscillator system. $\beta(j\omega)$ represents the voltage gain of the resonator while $A(j\omega)$ represents the voltage gain of the amplifier.

The configuration of a MEMS resonator based oscillator is as shown in Fig. 11. The voltage gain of the amplifier is given by $A(j\omega)$ and that of the resonator is given by $\beta(j\omega)$.

The closed loop voltage gain of the system is given by

$$A_{vf}(j\omega) = \frac{v_o}{v_i} = \frac{A_v(j\omega)}{1 - A_v(j\omega)\beta(j\omega)} \quad (27)$$

For oscillations to occur the loop gain of the system should be unity and the phase shift across the loop should be 0° or a multiple of 360° . These two conditions can be summarized in the following equation, which is the Barkhausen criteria.

$$\begin{aligned} A_v(j\omega)\beta(j\omega) &= 1 \\ \angle A_v(j\omega)\beta(j\omega) &= 0^\circ \end{aligned} \quad (28)$$

For developing a MEMS oscillator there exist two possible options: one based on the piezoresistive detection principle and the other based on the capacitive detection principle. Oscillator using the piezoresistive resonator has already been developed whereas the oscillator using the capacitive resonator has not yet been successfully developed. To develop an oscillator based on the capacitive detection principle it is necessary to overcome the following challenges.

- The resonance signal at the output of the resonator is very small. The signal strength is reduced further due to the presence of the bondpad at the output of the resonator. When such resonator is used to design an oscillator, the input bondpad of the amplifier comes in parallel with the output bondpad of the resonator and lowers the resonance signal further
- It is very difficult to develop a capacitive oscillator since the combination R_m and C_s is extremely critical and only at high voltage it satisfies the necessary condition to design an oscillator. The necessary condition for oscillation to occur in a

$$\text{piece topology is that the ratio } \frac{QC_m}{C_s} > 2 \text{ [12].}$$

To overcome the challenges of developing an oscillator based on the capacitive detection two solutions are proposed and are explained in more detail in the following sections.

B. Two chip oscillator design

By characterizing the existing resonators the electrical equivalent model of the resonators has been developed. To overcome the loading of the signal as a result of the parallel combination of the two bondpad impedances a buffer stage is introduced. Since JFET is the simplest transistor to be fabricated in the existing process flow of the resonators, a buffer stage using these JFET's has been designed and fabricated along with the resonators. The main purpose of the voltage buffer is to buffer the signal so that it can be connected to the input bondpad of the amplifier. The output bondpad of the resonator has been replaced by the JFET buffer stage since the connection from the resonator to the JFET buffer is made using a direct contact.

C. Single chip oscillator design

The solution proposed in the earlier design is a two-chip system in package solution for MEMS oscillator. However a new design for a MEMS oscillator is developed, which has not been reported in the literature before. In this design both the MEMS resonator and the amplifier are designed on the same chip. This makes it a single chip system in package MEMS oscillator. The characterization results of the previous resonator design have been used as a reference for developing the electrical model of the resonator. The simulation results determine the specification for the amplifier design. The gain of the resonator at the frequency of 25.85 MHz is -18 dB and the phase of the signal is 8° .

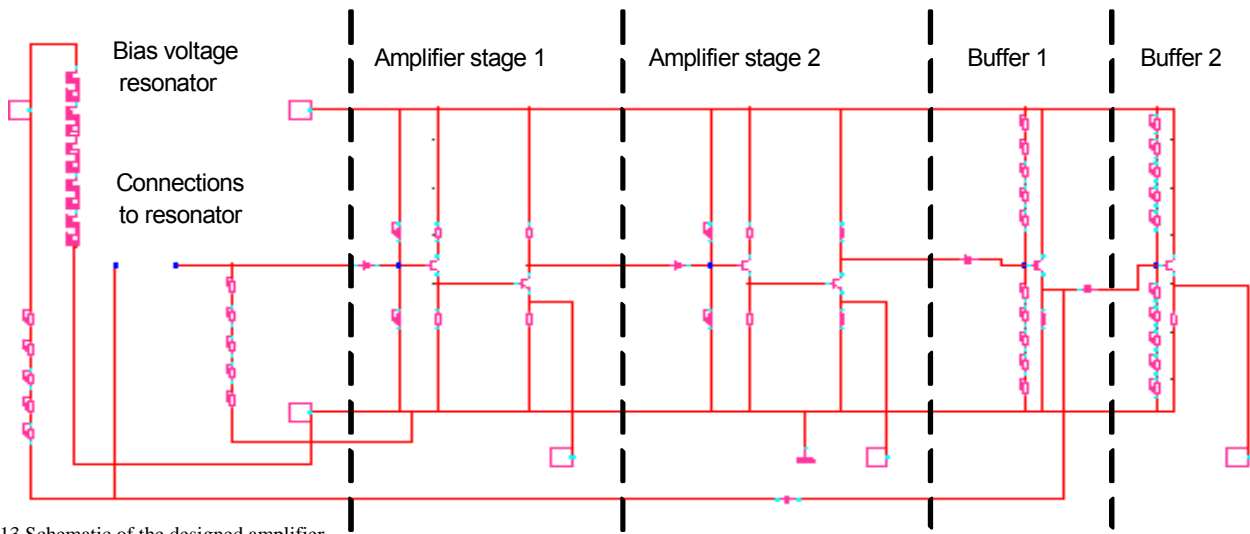


Fig 13 Schematic of the designed amplifier

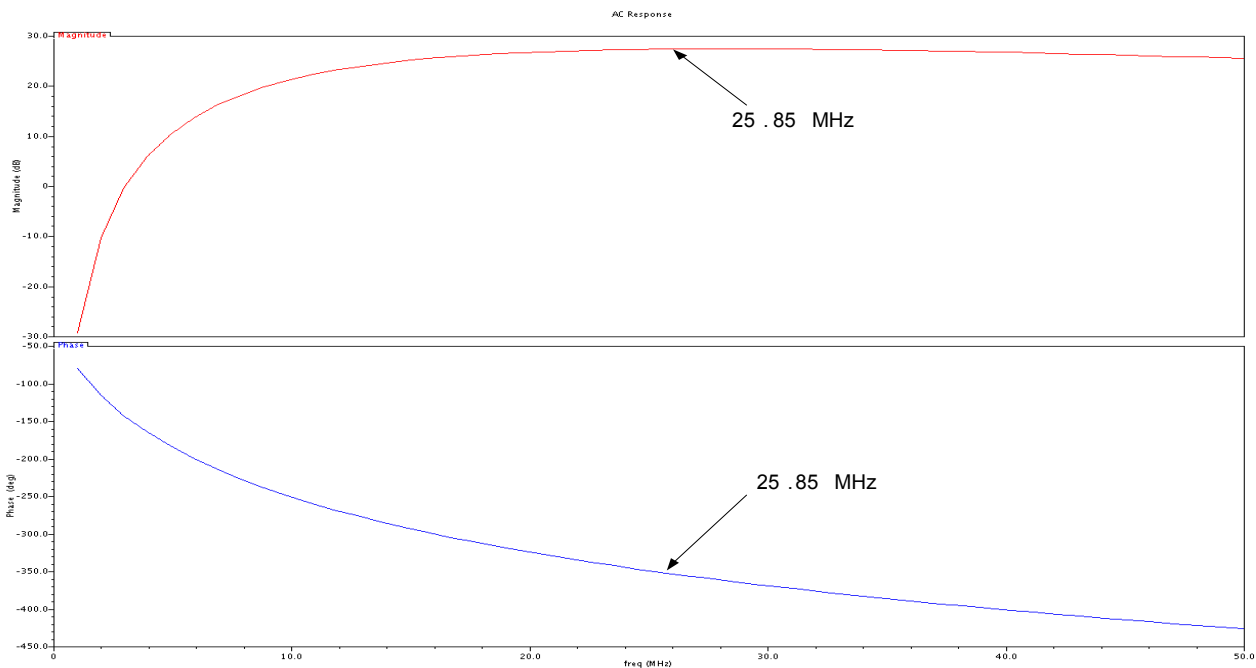


Fig 14 Frequency response of the designed amplifier

The schematic of the designed amplifier is shown in Fig. 13. The amplifier consists of two CC-CE amplifier stages cascaded using a capacitive coupling. The two stages are identical. The two amplifier stages are followed by two buffer stages. Buffer 1 is used to buffer the signal at the output of the second amplifier stage. It feeds back the amplified signal to the resonator. Buffer 2 is used to buffer the oscillation signal when connected to a spectrum analyzer with a 50Ω termination resistance. In the feedback path a decoupling capacitance is used to isolate the amplifier from the high dc bias voltage of the resonator.

The amplifier is designed to provide at least a gain of +18 dB and a phase shift required to satisfy the Barkhausen criteria

mentioned in equation (28). The frequency response of the designed amplifier is shown in Fig. 14. From the frequency response it can be seen that the gain of the amplifier at a frequency of 25.85 MHz is 27.5 dB. The gain of the amplifier is much higher than the required gain. In case of the designed MEMS oscillator the input signal V_i shown in Fig. 12 is zero. The amplifier amplifies the noise signal from the resonator thus; higher gain results in smaller starting time or the rise time of the oscillations. The signal amplitude grows until the onset of circuit non-linearities. Due to these non-linearities the gain of the circuit decreases until $|A\beta| = 1$ and the Barkhausen criteria for sustaining steady oscillations is satisfied. The high Q-factor of the resonator leaves very small design margin for

The designed module of the single chip MEMS oscillator is

as shown in Fig. 15. The area of the module is 1.7 mm^2 . There are two MEMS oscillator designs on the right side of the module. On the top left side lies a resonator design for characterization purpose and on the bottom left is the design of the amplifier. The designed MEMS oscillator is not optimized for phase noise or power consumption since, functionality and proof of concept for a single chip MEMS oscillator was assigned the highest priority.

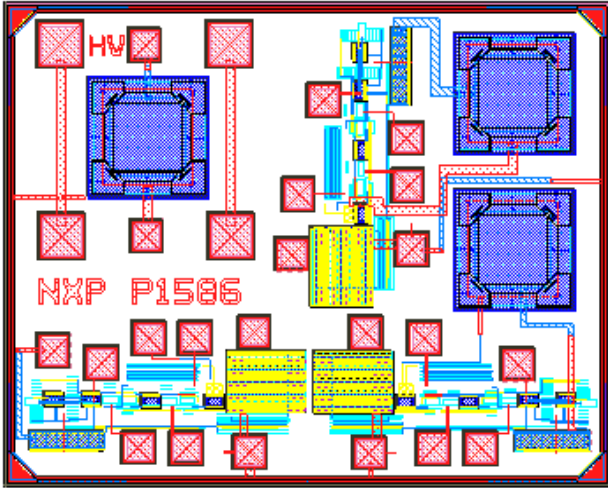


Fig. 15 Layout of the single chip MEMS oscillator module

VI. CONCLUSION

In this paper an electrical equivalent model of the MEMS resonator is presented. Dependencies of different model parameters on the frequency response of the resonator are verified by comparing the simulation and the measurement results. A parametric model has been developed and is used to identify the motional parameters along with the parasitic impedances of the resonator. The identified parameters have been used to develop an electrical equivalent of the MEMS resonator. This model has been used as a reference electrical model for developing an oscillator. For the first time a single chip MEMS oscillator based on the principle of capacitive detection is developed which operates at a frequency of 25.85 MHz. The designed oscillator is not optimized for phase noise or power consumption since proving functionality of a single chip MEMS oscillator was the main focus. However, in future the amplifier design can be improved for phase noise performance and power consumption so as to satisfy the stringent specifications for wireless application. The parametric model developed in this paper can be used as a basic model where temperature dependence and scaling of motional parameters can be included after analyzing the data from corresponding measurements. One of the principle highlights of this study has been the possibility to integrate a mechanical system and an electrical system on a single chip platform, which opens up enormous possibilities to integrate MEMS devices with electronic circuitry on a same platform.

APPENDIX

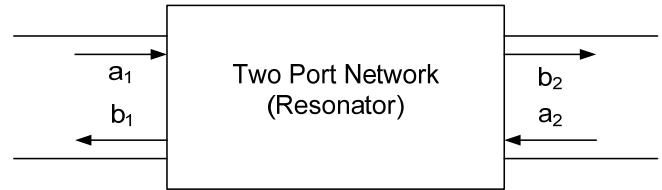


Fig. a Two-port S-parameter measurement

At high frequencies the behaviour of the signal can be approximated by travelling waves. The principle of S-parameter measurement can be explained from Fig. a. Two port S-parameters are defined considering a set of voltage waves. When a voltage wave from source is incident on a network a part of the voltage wave is transmitted whereas a part of the wave is reflected back towards the source due to mismatch in impedances. Similarly incident and reflected waves are present at the other port of the network. A set of variables can be defined by dividing the voltage wave with the square root of the reference impedance, the square of the magnitudes of the new variables are the traveling power waves. The two port S-parameter can be represented by the following matrix equality.

$$\begin{pmatrix} b_1 \\ b_2 \end{pmatrix} = \begin{pmatrix} s_{11} & s_{12} \\ s_{21} & s_{22} \end{pmatrix} \begin{pmatrix} a_1 \\ a_2 \end{pmatrix} \quad (29)$$

The network analyzer converts the voltage ratios in terms of the decibel ratios. Since the resonators are symmetrical network values of S_{12} and S_{21} which are the forward and the reverse transmission coefficients are similar. Similarly S_{11} and S_{22} , which are the forward and the reverse reflection coefficient, are similar.

ACKNOWLEDGEMENT

The author would like to thank Dr. ir. Jan-Jaap Koning and ir. J.J.M Bontemps, PDEng, of NXP Semiconductors, Prof. Dr. ir. P.P.J van den Bosch from TU Eindhoven (TU/e) for supervising this project and Dr. H. van der Vlist, groupleader Device Engineering and Characterization at NXP Nijmegen for the possibility to perform this Master graduation project. This project was a part of the Dutch MEMSland program.

REFERENCES

- [1] Wan-Thai Hsu and Minfan Pai, "The New Heart Beat of Electronics-Silicon MEMS oscillators," *Electronic Component and Technology Conference*, 2007, pp. 1895-1899.
- [2] T. Mattila, j. Kiihamaki, T. Lamminmaki, O. Jaakkola, P. Ranatakari, A. Oja, H. Seppa, H. Kattelus, I. Tittonen, "A 12 MHz micromechanical bulk acoustic mode oscillator" *Sens. Actuator A Phys.*, vol. 1, no. 1, pp. 1-9 2002.
- [3] D.W. Carr, S. Evoy, L. Sekaric, H.G. Craighead, J.M. Parpia, Measurement of mechanical resonance and losses in nanometer scale silicon wires, *Appl. Phys. Lett.* 75 (1999) 920.

- [4] T. Mattila, J. Kiihamaki, T. Lamminmaki, O. Jaakkola, P. Ranatakari, A. Oja, H. Seppa, H. Kattelus, I. Tittonen, "14 MHz micromechanical oscillator *Sens. Actuator A Phys.*, vol. 97, no. 98, pp. 497-502 2002.
- [5] S.Lee, M.U. Demirci, C.T.-C Nguyen, "A 10 MHz micromechanical resonator Pierce reference oscillator for communications, Digest of Technical Papers, Transducers'01, Munich, Germany, 2001, p. 1094.
- [6] C.T.-C Nguyen, "Frequency-selective MEMS for miniaturized low-power communication devices," *IEEE Trans. Microwave Theory Tech.*, vol 47, pp. 1486-1503, Aug. 1999.
- [7] Ville Kaajakari, Tomi Mattila, Aarne Oja, Jyrki Kiihamaki, Heikki Seppa, "Square-extensional mode single-crystal silicon micromechanical resonator for low-phase-noise oscillator applications," *IEEE Electron Device Letters*, vol.25, NO. 4. April 2004.
- [8] J.J.M. Bontemps, "MEMS resonator, concept or market product? ", Eindverslagen Stan Ackermans Instituut, ISBN 90-444-0598-6, 2006.
- [9] J.T.M van Beek, P.G.Steeneken, B. Giesbers, "A 10 MHz piezoresistive MEMS resonator with high Q" *Philips Research Eindhoven* .
- [10] W.E.Newell, " Miniaturization of tuning fork," *Science*, vol. 161, no. 3848, pp. 1320-1326, Sept 1968.
- [11] Bongsang Kim, Matthew A. Hopcroft, Rob N. Candler, Chandra Mohan Jha, Manu Agarwal, Renata Melamud, Saurabh A. Chandorkar, Gary Yama and Thomas W. Kenny, "Temperature dependence of Quality factor in MEMS resonator." *IEEE Journal of Microelectromechanical systems* vol. 17 no. 3 pp. 755-766, June 2008.
- [12] E.A. Vittoz, M.G.R. Degrauwe and S. Bitz, "High-performance crystal oscillator circuits: theory and application," *IEEE Journal of solid-state circuits*, vol. 23 no.3, pp 774-783, June 1988.